TITLE: In-situ plasma processing to increase the accelerating gradients of SRF cavities

PRIMARY AUTHOR: Marc Doleans

INTRODUCTION

A new in-situ plasma processing technique is being developed at the Spallation Neutron Source (SNS) to improve the performance of the cavities in operation. The technique utilizes a low-density reactive plasma at room-temperature to remove top-surface hydrocarbons. The plasma processing technique increases the work function of the cavity surface and reduces the overall amount of electron activity during cavity operation; in particular it increases the field-emission onset, which enables cavity operation at higher accelerating gradients. In this article, the main developments and results from the plasma processing R&D are presented and experimental results for in-situ plasma processing of dressed cavities in the SNS horizontal test apparatus are discussed.

FIELD EMISSION AND END-GROUP THERMAL INSTABILITY LIMITING THE ACCELERATING GRADIENTS IN THE SNS LINAC

Field emission in superconducting radio-frequency (SRF) cavities is a well-known limiting factor for operation at high accelerating gradients [Led, Pad, Sch]. Beyond certain electric field thresholds, the electrons from the metal surface of the cavity have a non-negligible probability of tunneling out. The field emitted electrons are accelerated by the stored electromagnetic fields in the cavity and subsequently deposit their energy by collision with the cavity radio-frequency (RF) surface leading to vacuum activity, increase of the surface temperature and Bremsstrahlung radiation. If the deposited energy-density is larger than the cooling capacity it can also lead to thermal breakdown of the superconductivity.

In the SNS superconducting linac (SCL), the end-groups, i.e. extremities of the accelerating cavities, are particularly prone to thermal instabilities since they are not actively cooled by liquid Helium but rather by conduction from the adjacent end-cells [Kim1]. Experimental evidence has shown that field emission at the SNS is the main limiting factor for reaching higher accelerating gradients in operated cavities [Kim2]. Figure 1 shows the accelerating gradient and peak surface electric field of all 81 cavities (33 medium-beta cavities and 48 high-beta cavities) at 60 Hz operation in the SNS linac. The average operating accelerating gradient for the two cavity geometries at the SNS is 12.0 and 13.0 MV/m respectively. The corresponding average peak surface electric fields are 32.4 and 35.1 MV/m. The average accelerating gradient for radiation onset is 11.2 MV/m for medium-beta cavities and 9.3 MV/m for high-beta cavities. The radiation originates from electron activity due to multipacting and field emission.

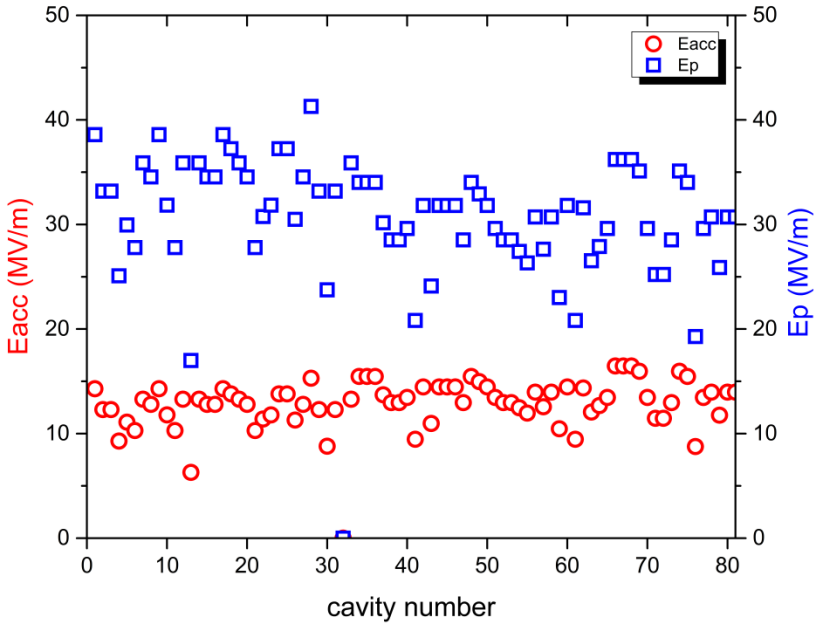

Figure 1: Accelerating gradient (Eacc) and peak surface electric field (Ep) of SNS cavities in operation at 60Hz repetition rate

The field emitted current density in the tunneling regime follows the Fowler-Nordheim equation [Wan]

$$J = a\frac{(\beta E)^2}{\phi} e^{-b\frac{\phi^{3/2}}{\beta E} + \frac{c}{\phi^{1/2}}} \qquad (1)$$

where a=1.54 x 10^6, b=6.53 x 10^3 and c=10.4 are constants, E is the electric field at the cavity surface in MV/m, β is the field-enhancement factor, ϕ is the surface work function in eV and J is the current density in A/m^2 . The most important feature of the field emitted current is its exponential dependence on the electric field. Once the field emission onset is reached, further increase of the accelerating gradient becomes increasingly difficult, especially for high duty-factor operation. The field emission onset gradient is defined as the electric field level leading to measurable field emitted current or related radiation.

INCREASING THE WORK FUNCTION TO INCREASE THE ACCELERATING GRADIENT

To mitigate field emission one can minimize the peak surface electric field for a given accelerating gradient, decrease the enhancement factor, or increase the work function.

Minimizing the ratio of the peak surface electric field and accelerating gradient is part of the design optimization of an RF structure. The physics behind the field enhancement factor is still an active topic of research but avoiding microprotrusions from the cavity surface is important during cavity fabrication,

particularly in the high surface electric field regions of a cavity. For cavities in operation at the SNS, a new in-situ plasma processing technique aims at increasing the work function of the cavity inner surfaces to reduce field emission and increase stable accelerating gradients. Based on Equation (1), the variation of the field emitted current density is given by

$$dJ = \partial_E J dE + \partial_\phi J d\phi \tag{2}$$

The field emitted current remains constant when dJ=0. After explicitly calculating the partial derivatives it leads to

$$\frac{dE}{E} = \frac{3}{2}\frac{d\phi}{\phi}\left(\frac{1+2\varepsilon/3+c\varepsilon/3\phi^{1/2}}{1+2\varepsilon}\right) \tag{3}$$

where the parameter epsilon is defined as $\varepsilon=\beta E/b\phi^{3/2}$. In good approximation for SRF cavities $\varepsilon<<1$ (e.g. $\varepsilon=0.04$ for $\beta=50$, E=50 MV/m and $\phi=4.3$ eV) and since the accelerating gradient E_{acc} is proportional to the surface electric field E it leads at first order to

$$\frac{dE_{acc}}{E_{acc}} = \frac{3}{2}\frac{d\phi}{\phi}\left(1+\varepsilon\, f(\phi)\right) \tag{4}$$

where the function $f(\phi)$is given by

$$f(\phi) = \frac{c}{3\sqrt{\phi}} - \frac{4}{3} \tag{5}$$

Equation (4) and (5) are based on the Fowler-Nordheim equation for field emission in DC fields given in Equation (1). But, using the equation for field emission in RF fields from [Wan] yields the exact same result to first order. For the case with $\beta=50$, E=50 MV/m and $\phi=4.3$ eV, the first order term is only 1.5% of the zeroth order value. Thus, the zeroth order approximation is sufficient in most cases:

$$\frac{dE_{acc}}{E_{acc}} = \frac{3}{2}\frac{d\phi}{\phi} \tag{6}$$

One concludes that for a cavity performance limited by field emission, increasing the cavity surface work function by 10-20% could lead to a 15-30% increase in the accelerating gradient.

HYDROCARBON CONTAMINATION DEGRADES THE WORK FUNCTION OF NIOBIUM SURFACES

The average work function of polycrystalline Niobium reported in the literature is 4.3 eV [Mic]. It is worth noting that the work function for Niobium has an unusually large dependence on its crystal structure, with literature reporting up to 0.8-0.9 eV spread [Mic, Ven]. Due to its strong affinity with oxygen, the Niobium surface typically has a 5 to 10 nm thick Niobium oxide layer, with Nb_2O_5 as its outmost layer. The work function of the Niobium pentoxide reported in the literature is 5.2-5.3 eV [Dac], while the lower oxides have smaller work functions, for example 4.2 eV for NbO [Gao]. Surface oxidation, dislocations, contaminants, and adsorbates at cryogenic temperature can change the work function and affect the field emission process [Bag, Bal, Liw]. Thus, the work function for the surface of cavities in operation is difficult to know in practice.

Residual gas analysis of thermally cycled cryomodules at the SNS have shown evidence of volatile hydrocarbons being released from the inner surfaces of cavities, in addition to expected gases such as nitrogen, oxygen, water, argon and carbon dioxide found in air. Figure 2 shows the partial pressure of various masses measured during the warm-up sequence of the cryomodule CM012 at the SNS from 2K to room-temperature using a residual gas analyzer (RGA) [Srs]. Hydrogen (H_2), methane (CH_4) and ethylene (C_2H_4) were identified from their mass, fragmentation patterns in the RGA and from the temperature at which they were released from the surface [Hon, Mks, Srs].

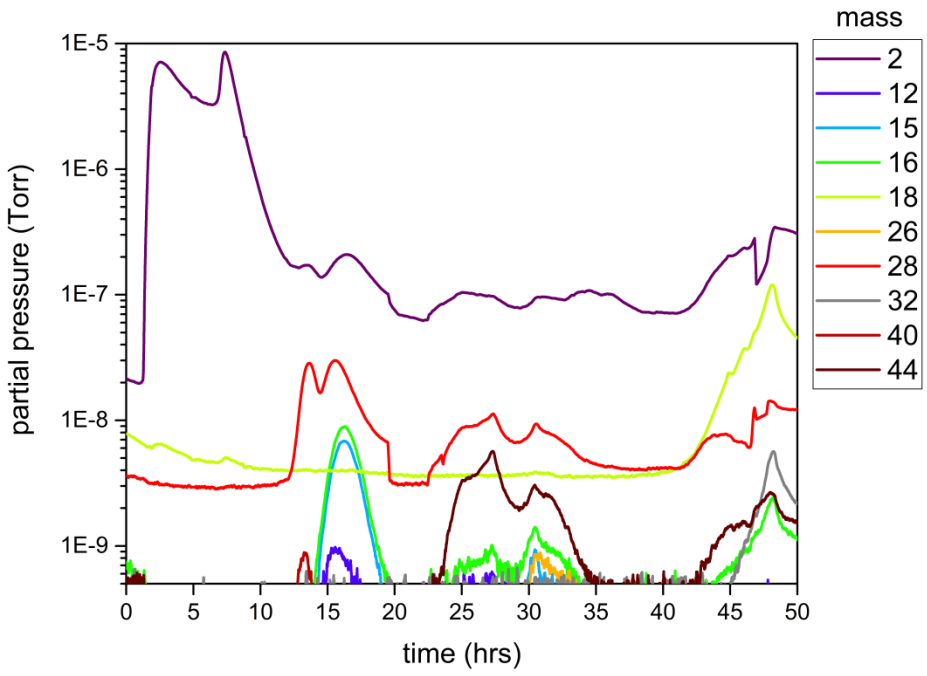

Figure 2: Residual gas analysis during warming up of the cryomodule CM012 at SNS from 2K to room temperature. Hydrocarbons such as methane (mass 16 at the 16 hour mark) and ethylene (mass 28 at the 31 hour mark) are released from the cavity surfaces.

All RGA signals measured during thermal cycling of cavities must come either from released gases that were condensed on the surface at cryogenic temperature or from volatile species produced on the surface during cavity operation for example by the interaction of electrons with surface contaminants [MaQ]. The exact initial chemical composition and bonding strength of hydrocarbons on the SNS cavity surfaces are not known so far, but evidence of hydrocarbons on other cavities have been reported in the literature [Cao, Dac, MaQ].

SIMS (secondary ion mass spectrometry) measurements of niobium samples fabricated for plasma-surface studies at the SNS also showed evidence of hydrocarbons at and near the metal surface. SIMS is a very sensitive surface analytical technique in static mode and can also provide depth composition in dynamic mode [Fri, Sai]. An example of depth profiling of a mechanically polished niobium sample is shown in Figure 3. Ions possibly related to hydrocarbon fragments, H^- and CH^-, are significantly concentrated at and near the top surface. Oxygen is also present at the top surface due for example to absorption of moisture on the sample.

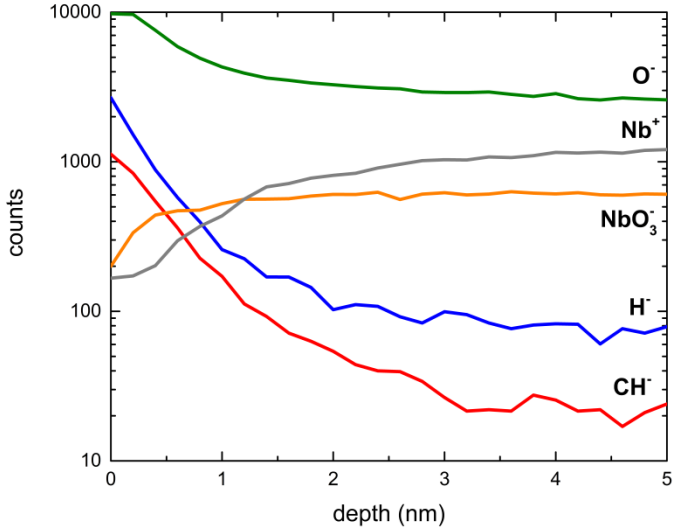

Figure 3: Secondary ion mass spectrometry depth profiles for various compounds on a niobium sample. Ions possibly related to hydrocarbon fragments, H^- and CH^-, are significantly concentrated at and near the top surface. Signals from ions related to niobium and niobium oxide are also shown.

The exact chemical form, bonding strength and effect on the work function for carbon and hydrocarbon compounds on transition metals is a very rich and complex topic [Got, Ost, Sam, Ton, XuL]. To estimate how hydrocarbon contaminants can affect field emission for SRF cavities, the work function of niobium samples with hydrocarbons at the top surface was measured and compared to work function of the niobium oxide. The work function was measured using the Kelvin Probe method. General information about this technique can be found here [Bai, Lag]. Measurements on mechanically polished and buffered chemical polished niobium samples using a 2 mm diameter probe revealed that the work function is typically 4.5-4.8 eV, lower than the expected work function of the niobium pentoxide. The

presence of carbon and hydrocarbon contaminants on top of niobium samples and their possible adverse effect on the work function and cavity performance have also been reported in other studies [Cao, Dac]. For example, the work function of the top carbonaceous layer estimated through XPS studies was reported at 3.6 eV [Dac]. Thus, the hydrocarbon contamination is believed to lower the work function of the niobium surface and be an aggravating factor for field emission. Removing the hydrocarbon contamination using the in-situ plasma processing technique can help increasing the surface work function and the accelerating gradient for cavity performance limited by field emission.

The source of the hydrocarbon contamination on niobium is not precisely known so far. But, hydrogen has a high solubility in niobium as in most metals [Jou, Vol] and hydrogen contamination occurs for example from adsorption of moisture on the surface and during chemical etching [Asp]. During surface studies it has been observed that carbon monoxide could be a source of carbon contamination. Interaction of carbon monoxide with transition metals is a well-known phenomenon [Mcc, Fie] and it is believed that dissociative chemisorption of carbon monoxide can occur when clean Niobium surface is exposed to air for example during assembly work in cleanroom.

IN-SITU PLASMA PROCESSING TO IMPROVE ACCELERATING GRADIENTS

Multiple campaigns of RF conditioning of SNS cavities at cryogenic temperature were conducted at the SNS over the first few years of operation and the accelerating gradient for each cavity was determined empirically for highest energy gain and stable operation [Kim1, Kim2]. The gradients haven't varied significantly since then but extensive progress in the understanding and use of sub-systems such as cold-cathode gauges and beam loss detectors have contributed to make the overall SCL operation remarkably reliable for a machine of its complexity.

Performance degradation has been observed for some cavities during operation [Kim3] but the performance is typically recovered by thermal cycling the corresponding cryomodule. The degradations have been mainly correlated to vacuum activity generated for example by errant beam striking the cavity surface [Pet] or to a gas burst from an ion pump adjacent to the modules. At present, the final beam energy is 940 MeV with the last cavity kept as energy reserve during operation allowing the linac final energy to be kept constant throughout a run even when some upstream cavity gradients need to be reduced.

To reach the design beam energy of 1 GeV and to provide operational margin for stable operation at the design beam power of 1.4 MW at the SNS [Neu], new cryomodules could be added or some existing cryomodules could be taken out of operation for refurbishment. Both of these options are costly and time consuming. The development of an in-situ plasma processing technique for cleaning of the surface hydrocarbons was pursued and regarded as a possible cost effective option.

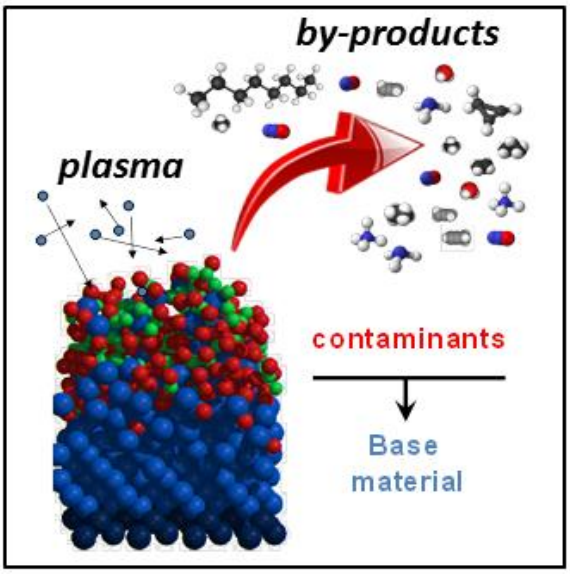

Figure 4: Basic concept of plasma surface interaction to clean surface from contamination.

Various types of plasma cleaning techniques have been developed for other processes; see the following references for examples [Ant, Aro, Haa]. In the present case, reactive species of the plasma interact with surface hydrocarbons and generate volatile by-products that can be removed by vacuum pumping. The basic concept for plasma cleaning of surface contaminants is shown in Figure 4. The newly developed plasma processing technique for SRF cavities is very different than the Helium processing technique [Ree, Sch]. Plasma processing is done at room temperature using a chemically reactive plasma, with gas pressure around 100 mTorr and electric field level in the order of 0.01 MV/m. Helium processing is done at cryogenic temperature using inert gas, with gas pressure around 0.1 mTorr and electric field level in the order of 10 MV/m.

The plasma processing R&D at the SNS is being conducted in four phases illustrated in Figure 5. The first phase uses offline undressed cavities to determine basic plasma processing parameters and develop a reliable plasma processing procedure for the SNS 6-cell cavities. The second phase conducts in-situ plasma processing of cavities in the horizontal test apparatus (HTA) which allows testing of single dressed cavities in a cryomodule-like environment with added instrumentation capability [Deg]. The third phase is the plasma processing of offline cryomodules and their concomitant testing in the SNS RF Test Facility. The last phase is the deployment of the in-situ plasma processing technique to cryomodules directly inside the SNS linac tunnel. Results from the first two phases are reported in this article. Work pertaining to the third phase is on-going and the start of the fourth phase is planned within a year.

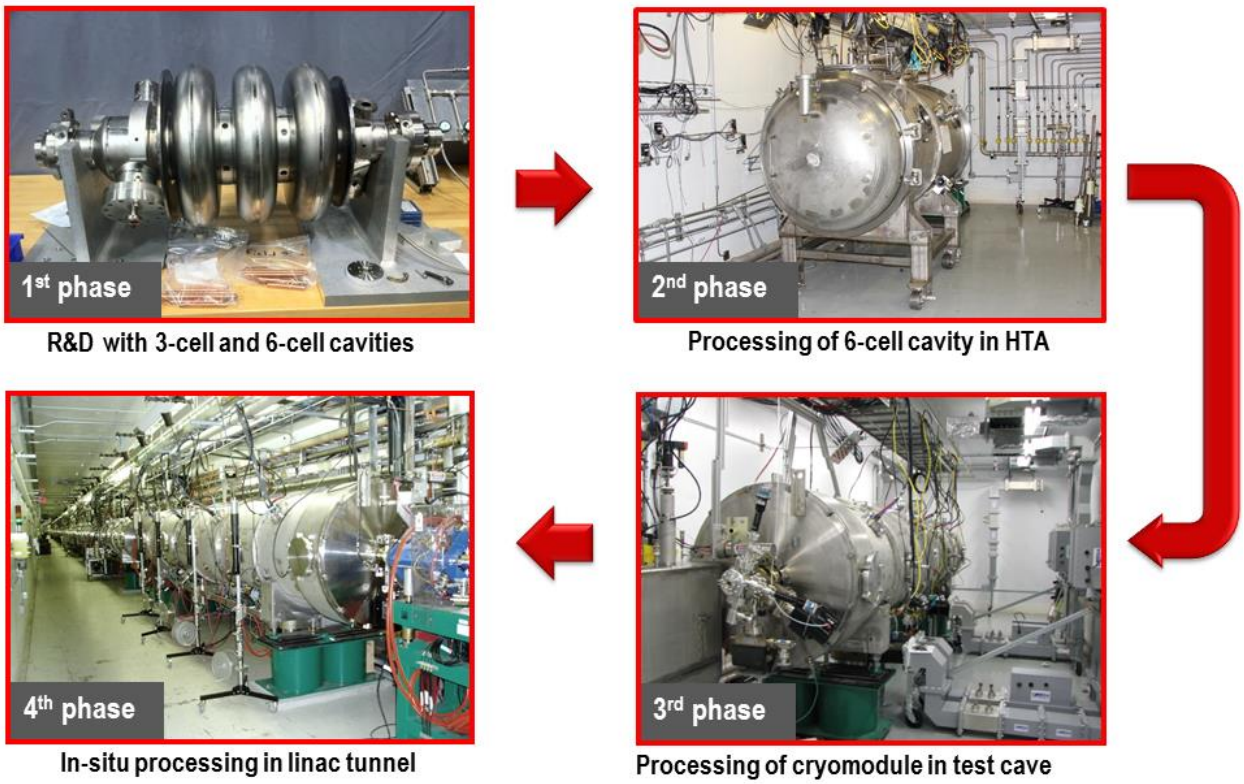

Figure 5: Four phases of R&D to develop and deploy a reliable in-situ plasma processing technique at the SNS.

PLASMA GENERATION IN SNS CAVITIES

A technique to reliably generate a low-density plasma at room-temperature in SNS high-beta cavities has been developed at the SNS [Dol]. Because the technique eventually needs to be applied to cavities directly in the SNS linac, constraints were applied to these studies such as using the same fundamental power coupler as operating cavities.

For the plasma processing, a continuous flow of process gas is generated through the cavity volume by injecting gas at one end of the cavity and vacuum pumping at the other end. For basic plasma ignition and tuning, pure neon gas is used. Neon gas was found to be adequate as it is easy to pump at the operating pressure (~100 mTorr), is chemically inert, provides a bright optical signal in the visible spectrum for monitoring, and provides good stability during the plasma tuning process. The average plasma electron temperature and density in the cavity volume haven't been directly measured but are estimated to be at the low-end of typical low pressure glow discharges ~eV and 10^{13} m^{-3} [Lie]. A typical set-up for plasma processing of an offline cavity is shown in Figure 6.

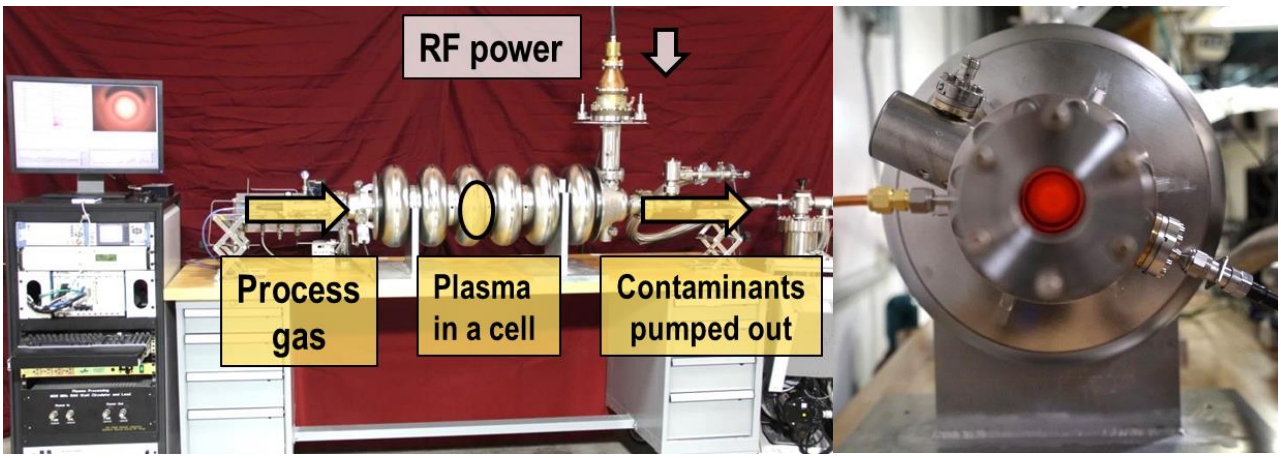

Figure 6: Set-up for plasma processing of an undressed SNS high-beta cavity (left). Image of a neon plasma inside an SNS cavity from a beam axial port (right).

The plasma is ignited in the cavity volume by exciting the passband modes of the 6-cell cavity and generating enough electric field to initiate a glow discharge, typically 10 kV/m at the cavity surface is required at 100 mTorr pressure. An RF station using a 500 W solid state amplifier was designed and constructed specifically for the plasma processing of SNS cavities. The RF station has a circulator and a load enabling stable operation even in full reflection mode. The amplifier has a central frequency of 805 MHz and a 25 MHz bandwidth, larger than the 11 MHz total spacing between the first and the last mode of the cavity fundamental passband. Thus, any of the passband modes can be used for igniting the plasma. The plasma typically ignites in the cell where the electric field is the highest and subsequently perturbs the mode frequencies and eigen vectors. The RF station uses two RF generators allowing simultaneous excitation of different modes and greater flexibility for tuning of the plasma. A plasma tuning technique has been developed to ignite and tune the plasma in any of the six cells of the SNS HB cavities. Some aspects of the plasma tuning in multicell RF cavities can be found in [Dol].

To date, the plasma processing technique has been applied successfully to six high-beta cavities, four undressed cavities on the workbench and two dressed cavities in the HTA. The plasma is sequentially ignited in each of the cells of a cavity and ignition in the fundamental power coupler (50 Ohm coaxial type) is avoided as it can damage its integrity for example by sputtering conductive material on the RF window. Figure 7 shows images of a neon plasma ignited in each cell of a high-beta cavity. The plasma is imaged by cameras positioned on the beam axis at each end of the cavity. The top row shows images taken by the camera mounted on the left port while the bottom row shows pictures taken by the camera mounted on the right port. Thermocouples mounted on the outside surface didn't indicate any temperature increase of the niobium surface due to the plasma inside the cavity volume.

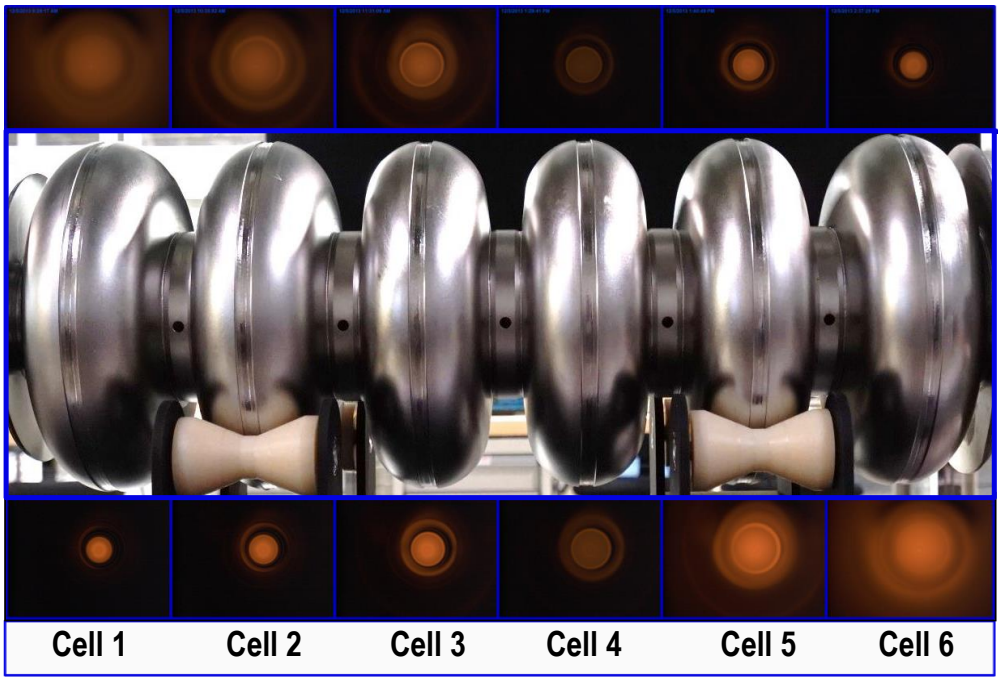

Figure 7: Neon plasma inside the cavity volume ignited sequentially in each of the six cells of an SNS high-beta cavity. Top row are images from a camera mounted on the left beam axial port, bottom row are images from a camera mounted on the right beam axial port.

PLASMA MIXTURE TO CLEAN RESIDUAL HYDROCARBONS

After the neon plasma is ignited and tuned into the desired cell, oxygen is introduced into the mixture at the percent level. Oxygen plasma has been used in various other applications for processing of hydrocarbons, see for example [Tsa,Vuj]. Reactive oxygen species of the plasma oxidize surface hydrocarbons and form volatile by-products: H_2, H_2O, CO and CO_2 [Fri]. The by-products of the plasma-surface reactions are pumped out and monitored using an RGA as shown in Figure 8. As illustrated, the amount of reaction by-products decreases over time as the surface is being depleted of hydrocarbons.

Based on the neon gas flow, q_{PV} [Ley], and on the RGA partial pressures it is possible to estimate how much carbonaceous material is removed by the plasma. The instantaneous $q_{PV,B}$ flow of a gas B based on the known $q_{PV,A}$ flow of a gas A and measured partial pressures P_A and P_B is given by

$$q_{PV,B} = q_{PV,A} \frac{P_B / s_B}{P_A / s_A} \qquad (7)$$

where S_A and S_B refer to the sensitivity of detection for both gases respectively. The sensitivity for the gases of interest, Ne, CO and CO_2 is mainly determined by the respective ionization cross sections in the RGA. Since the flow of each carbonaceous compound is not constant through time, one can average

their flow over the duration Δt of the plasma processing and use the ideal gas law to estimate the overall amount of matter removed

$$n = \frac{\overline{q_{PV}}\,\Delta t}{RT} \tag{8}$$

The average neon flow during the plasma cleaning was 50 sccm and using Equation (8) the total amount of CO and CO_2 collected was 8.9×10^{-6} and 9.0×10^{-6} mol respectively. The coverage at the surface in unit of monolayers is given by

$$\mathrm{cov} = \frac{n N_A}{N_m S} \tag{9}$$

where n is the quantity of matter in mol, N_A the Avogadro number, N_m the particle density for a monolayer on a surface estimated at 10^{19} m^{-2} and where S is the surface processed in m^2. Applying Equation (9) for the total amount of carbon collected from a single cell having a surface of about 0.17 m^2 leads to an estimate of 0.65 monolayer.

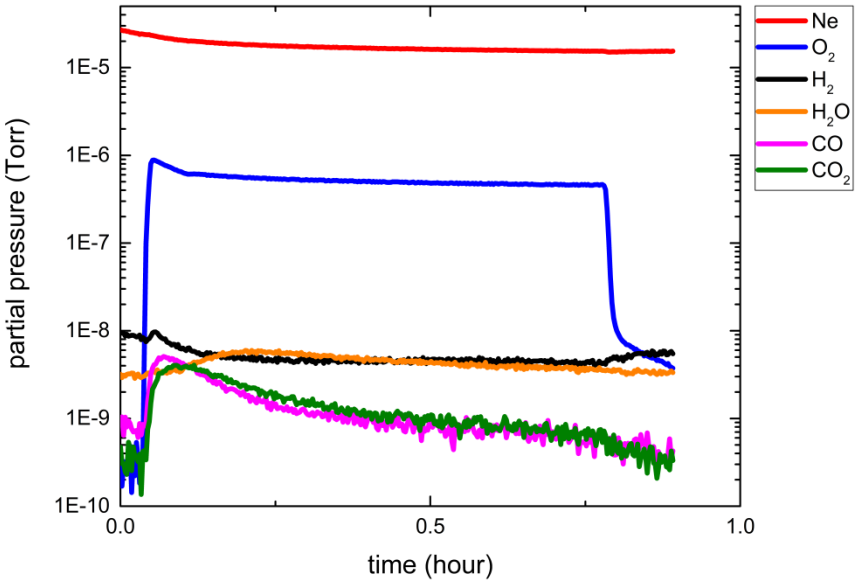

Figure 8: RGA signals during plasma processing of a cell from a HB cavity. A continuous flow of neon gas is maintained during the process and oxygen gas is introduced once the plasma is tuned into the desired cell. The oxygen is removed before the plasma is turned off. H_2, H_2O, CO and CO_2 are volatile by-products of reaction between the plasma and the hydrocarbons on the cavity surface.

The left panel of Figure 9 shows an example of RGA measurement during the plasma processing of a 6-cell HB cavity. All cells are processed sequentially. For clarity only the neon and carbon monoxide signals are shown. After all cells are plasma-cleaned, similar process is repeated and the result is shown in the

right panel of Figure 9. As illustrated the amount of residual hydrocarbons on the surface of each cell after the plasma cleaning is significantly reduced.

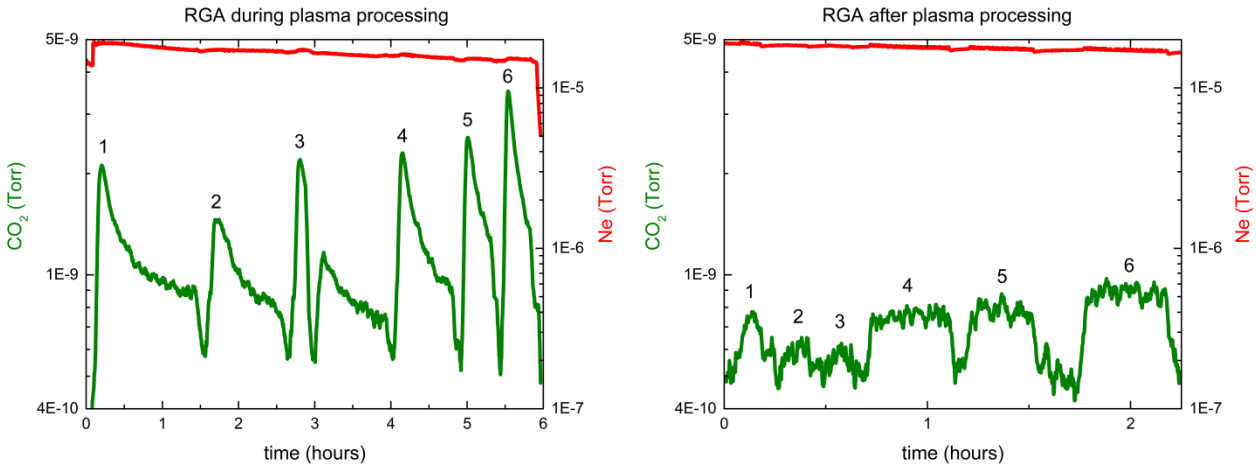

Figure 9: RGA signals of carbon dioxide and neon during the sequential plasma processing of the six cells of an SNS cavity (left). Similar RGA signals illustrate the reduction of hydrocarbon levels after plasma processing (right).

SIMS studies of plasma processed niobium samples confirm that the top surface hydrocarbons are being cleaned by interaction with the plasma. Example of depth profiles for the CH^- hydrocarbon fragment before and after a short plasma processing is shown in the left panel of Figure 10 for a processing using 5 minutes of active plasma over a 15 minute period. As expected, the concentration of CH^- at the surface is significantly reduced after the plasma cleaning with the neon-oxygen mixture. But, the hydrocarbons underneath the top surface weren't attacked by the short plasma processing.

Hydrogen and carbon can diffuse in niobium [Vas, Vol] and it was observed that hydrocarbons underneath the clean surface can migrate to the top surface over time. To mitigate this issue, subsequent plasma processing was determined to be effective. The right panel in Figure 10 shows the SIMS depth profile of the CH^- hydrocarbon fragment before and after plasma processing using 15 minutes of active plasma over a 3 hour period. As illustrated, the use of multiple steps of plasma cleaning over a longer period of time is an effective method to clean top surface hydrocarbons and below the surface hydrocarbons. Kelvin probe measurements indicate that such a methodology also leads to the highest increase in the work function of niobium samples.

The mobility for diffusion processes inside solids is governed by an Arrhenius-type equation and depends exponentially on the temperature. Thus, the mobility becomes negligible at cryogenic temperature. For this reason, migration of hydrocarbons from inside the material to the top surface should be negligible once the cavity is cooled down to operating temperature. Because the cool down process of a cryomodule takes time, it could be beneficial to do multiple plasma cleanings of the cavities over several days before the cool down sequence starts.

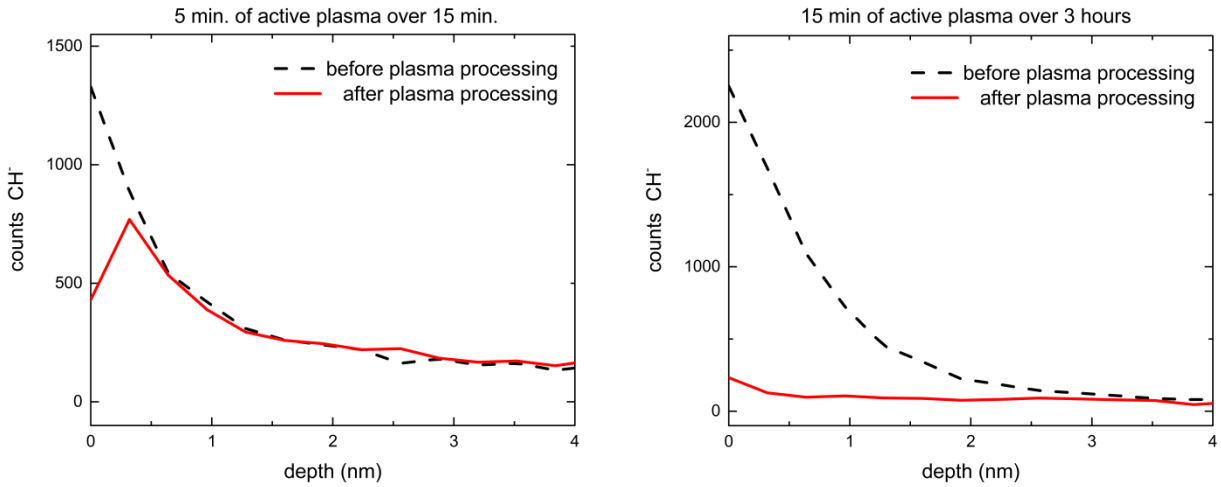

Figure 10: SIMS depth profiling on a niobium sample before and after plasma processing using 5 minutes of active plasma over 15 minutes duration (left). SIMS depth profiling on a niobium sample before and after plasma processing using 15 minute of active plasma over 3 hours duration (right).

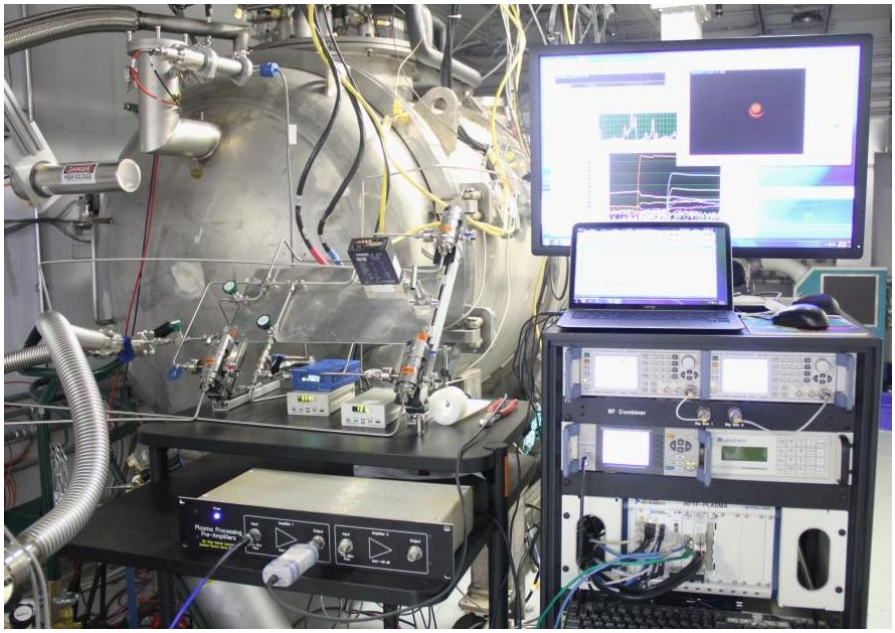

Figure 11: Plasma processing hardware adjacent to the HTA vessel. Imaging of the plasma and monitoring of RGA traces during the in-situ plasma processing can be seen on the screen of the RF station.

IN-SITU PLASMA PROCESSING AND COLD-TEST IN SNS HTA

Evaluation of the effect of the plasma processing technique on cavity performance was investigated using the HTA which allows testing of a single dressed cavity in a cryomodule-like environment [Deg]. The in-situ plasma processing technique was applied to two different dressed high-beta cavities in the HTA. In both instances, the cavity performance was evaluated at 4.5 K before and after plasma processing. Testing at 2K is planned in the near future. The plasma processing was done at room temperature between the two cold-tests. Figure 11 shows the plasma processing hardware adjacent to the HTA vessel in the SNS test cave. The HTA was cooled down using the SNS cryogenic test facility [How, XuT].

The two plasma processed cavities, HB52 and HB59, were spare cavities from the SNS project. Both were processed using buffered chemical polishing, dressed with a Helium vessel, cleaned and assembled in the HTA vessel in the SNS-SRF cleanroom. The final cleaning done on both cavities consisted of an ultrasonic cleaning in a mixture of ultra-pure water and micro-90 followed by a high-pressure rinsing with ultra-pure water.

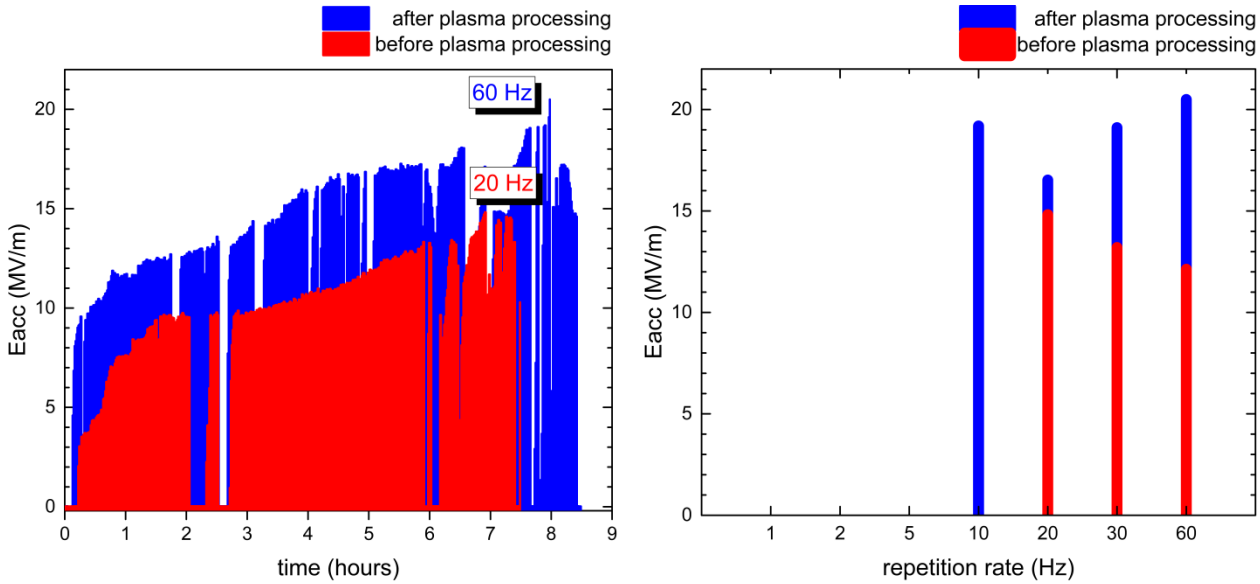

Figure 12: Cold-test results of HB59 cavity before and after plasma processing. Accelerating gradient over time (left) and accelerating gradient achieved at various repetition rates (right).

The HB59 cavity was tested before plasma processing and conditioned with high power RF for more than seven hours. The progression of the accelerating gradient throughout the conditioning process is shown in the left panel of Figure 12. During the conditioning, multipacting and field emission were both encountered and resulted in frequent vacuum activity, temperature increase and thermal breakdowns. The highest gradient reached was 15.2 MV/m at 20 Hz repetition rate. This gradient couldn't be sustained at 60 Hz, the nominal repetition rate of the SNS linac. Repetitive quenches were observed

around 15 MV/m. The accelerating gradients reached during the conditioning at various repetition rates are shown in the right panel of Figure 12.

After plasma processing at room temperature, the cavity was re-tested at 4.5 K. The RF conditioning was found to be substantially easier after plasma processing with milder vacuum activity and reduced temperature excursions. The accelerating gradient with respect to time and to the repetition rate after plasma processing is also shown in Figure 12. The highest gradient of 20.5 MV/m was achieved during operation at 60 Hz.

Radiation monitors used around the HTA measure the X-ray radiation associated with electron activity during the test. As expected from Equation (1), the field emitted electron current and thus the corresponding radiation level increases exponentially once the field emission regime is attained. The radiation per pulse is plotted with respect to the accelerating gradient in Figure 13. The measurable onset of field emission, i.e. radiation signal above noise level for the radiation detectors, increased from 12 MV/m before plasma processing to 14.2 MV/m after plasma processing.

Cavity HB59 was kept at room temperature for two months under argon atmosphere. It was subsequently plasma processed a second time and re-tested at cold. The performance of the cavity was improved further and the cavity accelerating gradient reached 22 MV/m with a field emission onset at 15.8 MV/m.

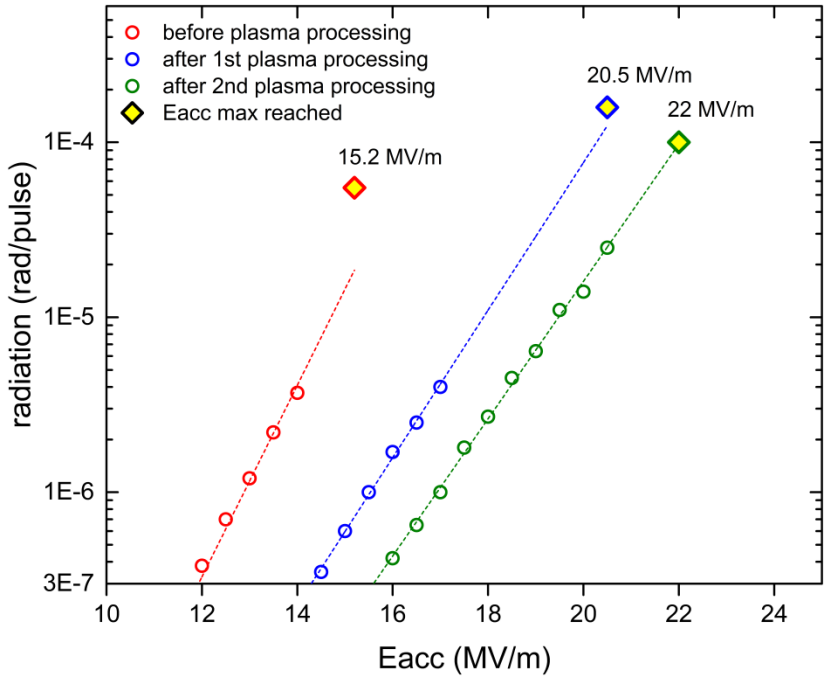

Figure 13: Radiation per pulse (log. scale) as a function of the accelerating gradient for the HB59 cavity. Dashed trend lines as well as the highest gradients achieved during each cold-test are shown.

Tests done on niobium samples indicate that for optimum removal of the hydrocarbon contamination and for the largest increase of the work function, multiple plasma cleanings over several days is preferable. Time between plasma cleanings allows below surface hydrocarbons to migrate to the top surface where they can be removed by the plasma. During the first plasma processing of HB59, each cell of the cavity was processed for thirty to forty minutes only. It is believed that this wasn't enough time for optimum cleaning of the cavity. It should be noted that the time scale of a few days is constrained by the migration process of hydrocarbons to the top surface and not by the cleaning of the surface by the plasma.

During surface studies on niobium samples, 0.7-1.0 eV increase of the work function has been measured after plasma processing. The initial work function of samples was typically 4.7 eV. Using these values in Equation (6) leads to an expected increase in the field emission onset of 22-32%.

For the HB59 cavity, the field emission onset has increased from 12 MV/m before plasma processing to 14.2 MV/m after the first plasma processing and to 15.8 MV/m after the second plasma processing, corresponding to a 18% and 32% increase in field respectively. Thus, the increase in the field emission onset obtained experimentally seems in reasonable agreement with the expected increase from surface studies.

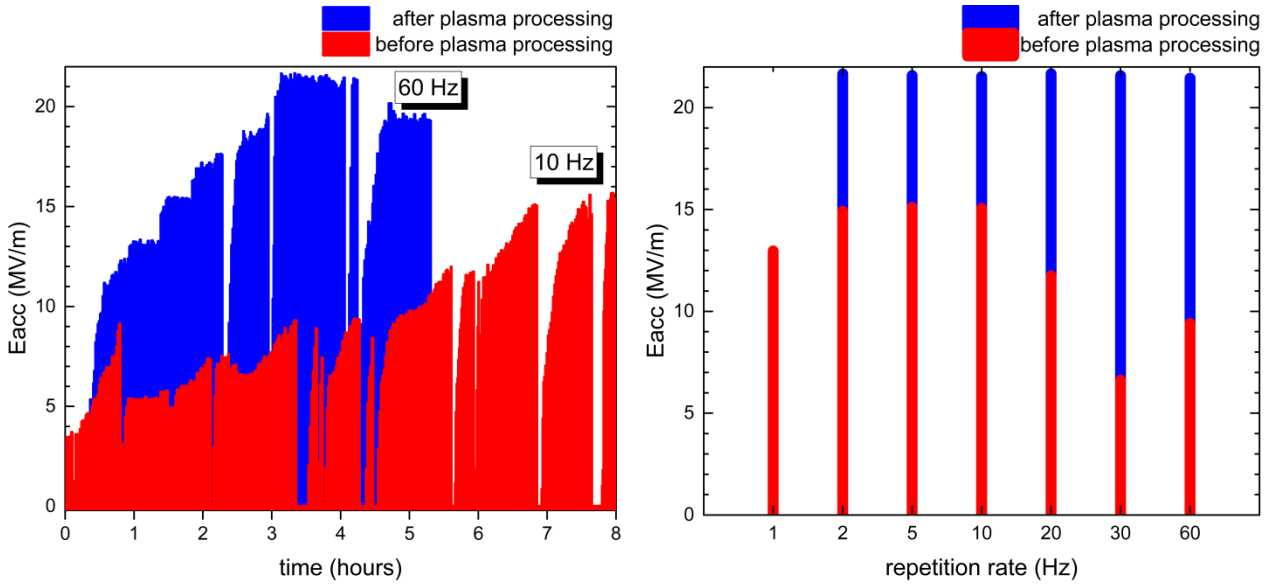

Figure 14: Cold-test results of HB52 cavity before and after plasma processing. Accelerating gradient over time (left) and accelerating gradient achieved at various repetition rates (right).

As done for HB59, the HB52 cavity was tested in the HTA with cold tests performed before and after plasma processing. For HB52, a plasma cleaning was conducted every day over four days. Each cell was plasma processed for about thirty minutes during each cleaning. The accelerating gradient with respect to time and to the repetition rate before and after plasma processing is shown in Figure 14. As for the HB59 cavity, the plasma processing improved the performance of the HB52 cavity.

SNS HB cavities always show broad multipacting activity for accelerating gradients between 9 and 14 MV/m. The 12 to 14 MV/m region is especially sensitive for SNS HB cavities because of the typical overlap of electron activities related to multipacting and field emission [Kim1, Kim2]. The severity of the multipacting activity varies from cavity to cavity but after some RF conditioning, the effect from multipacting typically reduces and the electron activity from field emission becomes the limiting factor for most SNS cavities. The cavity HB52 showed unusually severe multipacting activity during its first cold-test, but no evidence of field emission. Thus, the limiting factor for the accelerating gradients of HB52 and HB59 cavities were initially very different. HB59 was similar to most cavities in operation at the SNS and its accelerating gradient limited by electron activity from field emission while HB52 resembled other cavities in operation limited by severe multipacting.

After eight hours of tedious RF conditioning with significant vacuum activity and several quenches, the HB52 cavity could be operated at 15 MV/m at a repetition rate of 10 Hz. Higher repetition rates were seldom used due to thermal instability of the end-group on the fundamental power coupler side. The cavity performance was significantly improved after plasma processing. The cavity achieved a maximum gradient of 21.5 MV/m and could be run stably at 19.5 MV/m and 60 Hz.

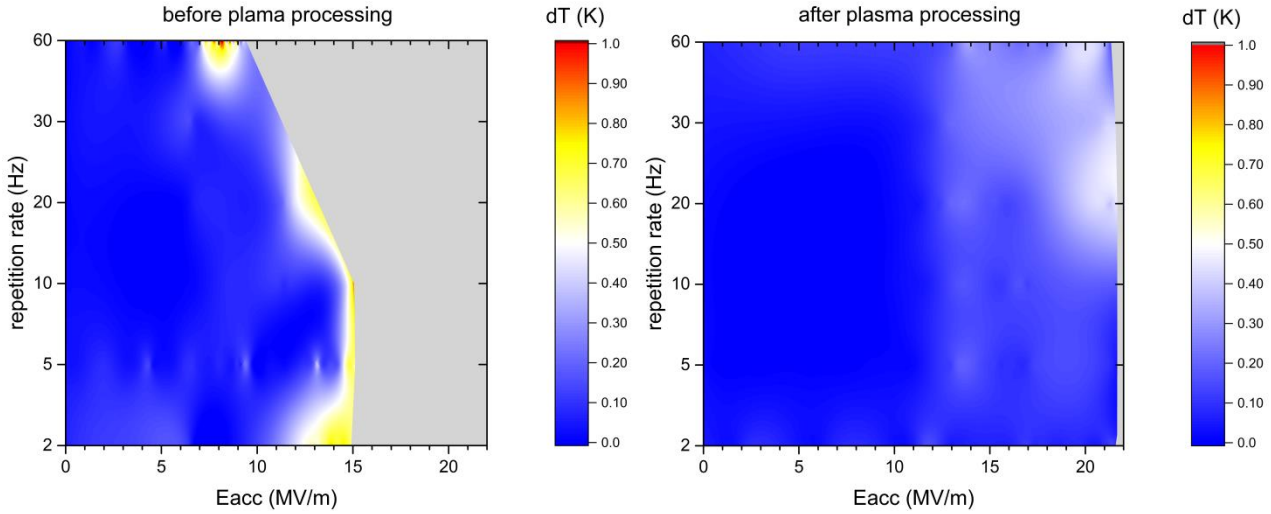

Figure 15: Temperature increase recorded during cold-tests of HB52 cavity before and after plasma processing. The temperature increase was recorded at various accelerating gradients and repetition rates. Lower increase in temperature was observed after plasma processing indicating milder electron activity in the end-groups. Gray areas indicate regions with no data.

A thermal diode mounted on the cooling circuit for the end-groups and RF coupler flange of the cavity recorded the thermal effect of the electron activity during both cold tests. The change in temperature as a function of the accelerating gradient and repetition rate is shown in Figure 15 before and after plasma processing. As illustrated, the thermal stability was improved after plasma processing, Lower temperature increase was observed during the test after plasma processing even though higher accelerating gradient was achieved.

The plasma processing had a positive impact on the HB52 cavity performance even though this cavity was limited by multipacting and not by field emission. The severity of the multipacting is strongly affected by the SEY (secondary emission yield) of the surface, and the SEY is affected by the escape probability of the electron and thus by the work function of the surface. For example, a study on the effect of work function on SEY of gold surface [caz] showed that an increase of the work function by 1 eV lowered the SEY by 50%. But, the increase of the work function of the niobium surface after plasma processing might not be the main factor reducing the multipacting severity. A study on niobium surfaces [Hil] showed that a contaminated layer composed of a mixture of hydrocarbons and water with a large intrinsic SEY of about 3 develops on samples exposed to air. The study concludes that an important fraction of the secondary electrons are generated within this contaminated layer, which leads to an increase in the SEY of the niobium surface. Thus, improvement of the SEY by plasma processing could be because of the increase of the work function and/or because of the removal of the hydrocarbon and water contaminated layer with large intrinsic SEY. Specific surface studies on the SEY of niobium surface before and after plasma processing are required to explore and understand the benefit of this new processing technique for cavities limited by multipacting.

CONCLUSION

A new In-situ plasma processing technique is being developed at the SNS to improve the performance of the cavities in operation. The technique utilizes a low-density reactive plasma at room-temperature to remove top-surface hydrocarbons and to increase the work function of the cavity surface. This procedure leads to an increase of the field emission onset and higher accelerating gradients. Cold-tests on dressed cavities after plasma processing demonstrated the improvement of performance for cavities limited by field emission but also by multipacting. Plasma processing of an offline cryomodule is planned next and deployment to cryomodule in operation will ensue.

REFERENCES

[Ant] A.B. Antipenkov, P. Ladd, R. Marrs, "ITER glow discharge cleaning system" Fusion Engineering and Design 56–57 (2001) 233–238

[Aro] B.-O. Aronsson, J. Lausmaa, and B. Kasemo, "Glow discharge plasma treatment for surface cleaning and modification of metallic biomaterials" J Biomed Mater Res. 1997 Apr; 35(1):49-73 http://www.ncbi.nlm.nih.gov/pubmed/9104698

[Asp] A. Aspart and C.Z. Antoine "Study of the chemical behavior of hydrofluoric, nitric and sulfuric acids mixtures applied to niobium polishing" Applied Surface Science 227 (2004) 17–29

[Bag] P. Bagus, D. Kafer, G. Witte, and C. Woll "Work function changes induced by charged adsorbates: Origin of the polarity asymmetry" Physical Review Letters **100**, 126101 (2008)

[Bai] I. D. Baikie, S. Mackerbzie, P. J. Z. Estrup and J. A. Meyer "Noise and the Kelvin method" Rev. Sci. Instrum. 62 (5), May 1991

[Bal] R. Ballantini, A. Daccà, G. Gemme, R. Parodi **"**Improvement of the maximum field of accelerating cavities by dry oxidation" Proceedings of the 1999Workshop on RF Superconductivity, La Fonda Hotel, Santa Fe, New Mexico, USA

[Cao] C. Cao et al. "Detection of surface carbon and hydrocarbons in hot spot regions of niobium superconducting rf cavities by Raman spectroscopy" Physical Review Special Topics - Accelerators and Beams 16, 064701 (2013)

[Caz] Jacques Cazaux "Calculated influence of work function on SE escape probability and Secondary Electron Emission yield" Applied Surface Science **257** (2010) 1002-1009

[Dac] A. Dacca, G. Gemme, L. Mattera, R. Parodi "XPS characterization of niobium for rf cavities" Proceedings of the 1997 Workshop on RF Superconductivity, Abano Terme (Padova), Italy

[Deg] B. Degraff et al., "Commissioning and operation of the horizontal test apparatus at SNS"

[Dol] M. Doleans et al., "Plasma processing R&D for the SNS superconducting linac RF cavities" Proceedings of the 2013 Workshop on RF Superconductivity, Paris, France

[Fie] André Fielicke et al.,"The adsorption of CO on transition metal clusters: A case study of cluster surface chemistry" Surface Science 603 (2009) 1427–1433

[FrA] A. Fridman "Plasma chemistry" Cambridge university press (2008) ISBN-13978-0-511-40243-2

[Fri] G. Friedbacher and H. Bubert "Surface and thin films analysis" Wiley-VCH (2011)

[Gao] W. Gao et al., "NbO as gate electrode for n-channel metal-oxide-semiconductor field-effect-transistors" Applied Physics Letters **84**, 4666 (2004) http://dx.doi.org/10.1063/1.1759780

[Got] Yasuhito Gotoh, Hiroshi Tsuji, and Junzo Ishikawa "Measurement of work function of transition metal nitride and carbide thin films" Journal of Vacuum Science & Technology B **21**, 1607 (2003) http://dx.doi.org/10.1116/1.1591749

[Haa] Tatsuya Hayashi and Hideaki Toya "Glow discharge cleaning of vacuum switch tubes" IEEE Transactions on Plasma Science, vol. 19, no. 5, October 1991

[Hil] N. Hilleret, C. Scheuerlein, M. Taborelli "The secondary-electron yield of air-exposed metal surfaces" Appl. Phys. A 76, 1085–1091 (2003)

[Hon] R.E. Honig and H.O. Hook, RCA Review, **21**, 360 (1960)

[How] M. Howell et al. "Status of Spallation Neutron Source Cryogenic Test Facility", Proceedings of PAC2013, Pasadena, United States (2013)

[Jou] K. jousten "Thermal outgassing" lecture notes from CERN accelerator school, Denmark (1999)

[Kim1] S-h Kim and I. Campisi "Thermal stabilities and optimal operating parameters for the Oak Ridge Spallation Neutron Source superconducting linear accelerator" Physical Review Special Topics – Accelerator and Beams **10**, 032001 (2007)

[Kim2] S-h Kim "Status of the SNS Superconducting Linac and Future Plan" Journal of the Korean Physical Society, Vol. 52, No. 3, March 2008, pp. 714-720 (2008)

[Kim3] S-h Kim "The status of the superconducting linac and SRF activities at the SNS" Proceedings of the 2013 Workshop on RF Superconductivity, Paris, France

[Lag] Bert Lägel "The application of the kelvin probe in materials science" Ph.D. Thesis (2000) Robert Gordon University

[Ley] W. Umrath et al. "Fundamentals of vacuum technology" Oerlikon Leybold vacuum 00.200.02, Kat.-Nr. 199 90 (2007)

[Led] S. Lederer, D. Reschke "Field emission in SRF cavities" Presentation at the Unwanted Beam Workshop, Humboldt-University Berlin, Germany, 17-18 December 2012

[Lie] M. A. Lieberman and A. J. Lichtenberg "Principles of plasma discharges and materials processing" John Wiley & Sons, Inc. 2005

[Mac] W. A. Mackie, L. A. Southall, Tianbao Xie, and G. L. Cabe, P. H. McClelland **"**Emission characteristics of NbC/Nb field emitter array cathodes" Journal of Vacuum Science & Technology B **21**, 422 (2003) http://dx.doi.org/10.1116/1.1527636

[Mcc1] E. M. McCash "Surface Chemistry" Oxford university Press, 2001. ISBN 0 19 850328 8

[MaQ] Q. Ma and R.A. Rosenberg **"**Thermal and electron-beam irradiation effects on the surfaces of Niobium for RF cavity production" Proceedings of the 2001 Workshop on RF Superconductivity, Tsukuba, Japan

[Mic] H. B. Michaelson "The work function of the elements and its periodicity" J. Appl. Phys. **48**, 4729 (1977) http://dx.doi.org/10.1063/1.323539

[Mks] MKS-Application Note, RGA Application Bulletin #208

[Neu] "Neutron sciences directorate five year plan 2012-2016", SNS-NSCD-EXE-PN-0001, R00 (2012)

[Ost] H. Ostrom, "Chemical bonding of hydrocarbons to metal surfaces" Ph.D. dissertation in Chemical Physics, Stockholm University (2004)

[Pad] H. Padamsee, J. Knobloch and T. Hays, "RF Superconductivity for accelerators" Wiley series in beam physics and accelerator technology, ISBN 0-471-15432-6

[Pet] C. Peters et al., "Superconducting radio frequency cavity degradation due to errant beam, proceedings of IPAC 2015, Richmond, Virginia, US

[Ree] C. E. Reece et al., "Improvement of the operational performance of the SRF cavities via in situ helium processing and waveguide vacuum processing" Proceedings of PAC97 conference, Vancouver, BC, Canada (1997)

[Sai] Scientific Analysis Instruments Limited, MiniSIMS TOF/alpha, user manual version 1.2

[Sam] G. V. Samsonov, I. A. Podchernyaeva, V. S. Fomenko, V. A. Lovrenko,, L. N. Okhremchuk, and T. G. Protsenko "Correlation between the work functions of transition metal carbides in their homogeneity regions and Surface Recombination of hydrogen atoms" Translated from Poroshkovaya Metallurgiya, No. 5 (113), pp. 62-66, May, 1972. Original article submitted May 10, 1971

[Sch] H. A. Schwettman, J. P. Turneaure, and R. F. Waites "Evidence for surface state enhanced field emission in rf superconducting cavities" Journal of Applied Physics 45, 914 (1974) http://dx.doi.org/10.1063/1.1663338

[Srs] Standford Research Systems, Residual gas analyzer RGA200, Operating Manual and Programming Reference, revision 1.8 (2009)

[Ton] A. Ya. Tontegode "Carbon on transition metal surfaces" Progress in Surface Science, Vol. 38 pp. 201-429 (1991)

[Tsa] C. C. Tsai et al. "Plasma surface cleaning in a microwave plasma source" ORNL/TM-12495, Oak Ridge Naitonal Laboratory library (1994)

[Vas] L. B. Vasilenok et al. "Diffusion of carbon along grain boundaries in niobium" Doklady Physics, Vol. 45, No. 11, 2000, pp. 588–591

[Ven] J. A. Venables “Introduction to surface and thin film processes” Cambridge University press (2000)

[Vuj] D. Vujošević et al. “Optical emission spectroscopy characterization of oxygen plasma during degradation of Escherichia coli” J. Appl. Phys. **101**, 103305 (2007); doi: 10.1063/1.2732693

[Vol] J. Volkl, G Schaumann and G. Alefeld “Diffusional relaxation of H and D in V and Nb” J. Phys. Chem. Solids Pergamon Press 1970. Vol. 31, pp. 1805-1809

[Wan] J. W. Wang and G. A. Loew “Field Emission and RF Breakdown in High-Gradient Room-Temperature Linac Structures” SLAC-PUB-7684 (1997)

[XuL] L. Xu, C. Wang, C. Q. Hu, Z. D. Zhao, W. X. Yu, and W. T. Zheng “Field electron emission enhancement of amorphous carbon through a niobium carbide buffer layer” Journal of Applied Physics **105**, 014302 (2009)

[XuT] T. Xu et al., “Status of Cryogenic System for Spallation Neutron Source’s Superconducting Radiofrequency Test Facility at Oak Ridge National Laboratory”, Advances in Cryogenic Engineering, AIP conference proceedings (2012)